

PHYSICAL METALLURGY
AND HEAT TREATMENT

Construction of Gallium–Tin Nonequilibrium State Diagram and Its Analysis

V. D. Aleksandrov^{a, *}, A. P. Zozulia^{a, **}, and S. A. Frolova^{a, ***}

^aDonbas National Academy of Civil Engineering and Architecture, Makeevka, 286123 Ukraine

*e-mail: avd-crystal@mail.ru

**e-mail: zozulyanastya@yandex.ua

***e-mail: primew65@mail.ru

Received January 5, 2019; revised May 12, 2019; accepted May 14, 2019

Abstract—Overcooling of gallium–tin alloys under normal conditions has been studied by thermal analysis. The following samples have been analyzed: Ga (I); two hypoeutectic alloys: 95% Ga + 5% Sn (II), 90% Ga + 10% Sn (III); eutectic alloy: 96.3% Ga + 13.7% Sn (IV); and five hypereutectic alloys with Sn content of 20% (V), 35% (VI), 50% (VII), 80% (VIII), and pure tin (IX). A nonequilibrium state diagram of this system is constructed. Herewith, the eutectic composition does not vary and the eutectic temperature decreases to 5.5°C, that is, 26°C below that of three-phase eutectic equilibrium. The eutectic temperature does not actually vary upon a variation of cooling rates of eutectic alloy from 0.06 to 60°C/min. It has been detected that a slight decrease in overcooling is expected in the hypoeutectic region, whereas in the hypereutectic region overcooling increases while the alloy composition approaches eutectic. Activities and activity coefficients of components on the lines of equilibrium and nonequilibrium liquidus have been calculated. It is demonstrated that the activities on the lines of both equilibrium and nonequilibrium liquidus decrease in a predictable manner, and the activity coefficients increase while the composition approaches eutectic. Concentration paths of equilibrium and nonequilibrium crystallization are shown in the state diagrams.

Keywords: gallium, tin, alloys, state diagram, melting, crystallization, thermal analysis, liquidus, solidus, eutectics, overcooling, activities, crystallization paths

DOI: 10.3103/S1067821220020029

INTRODUCTION

Gallium–tin alloys are widely used for the production of semiconductors and solar cells, for the fabrication of low temperature solders, for creating reference points aimed at the calibration of instruments [1–5], and so on. The efficiency of these alloys is determined by the methods of their production and solidification conditions [6]. It is important to reveal the conditions of one or another phase transition of alloys based on an analysis of equilibrium and nonequilibrium state diagrams.

Gallium–tin alloys form a diagram of eutectic type with the bilateral restricted solubility of components. Figure 1 illustrates Ga–Sn equilibrium diagram [6]. The hypoeutectic region contains an α solid solution based on gallium and the hypereutectic region contains a β solid solution based on tin. Therefore, the eutectic alloy below the temperature T_E is the mixture of α and β solid phases.

Various data are available concerning the composition of eutectics. According to [6], they are Ga + 8.5 mol % Sn with eutectic temperature $T_E = 20.5^\circ\text{C}$. According to [7], they are Ga + 5 mol % Sn and $T_E =$

20.0°C , according to [8] they are Ga + 8.5 mol % Sn and $T_E = 20.6^\circ\text{C}$, and according to [9] they are Ga + 7.8 mol % Sn and $T_E = 21.8^\circ\text{C}$.

Even higher differences are observed in the studies of overcooling of both gallium and tin as a function of overcooling rates, the thermal history of the melt, the weight of samples, and so on [10–13].

This work attempts to construct a nonequilibrium state diagram in the gallium–tin system with respect to liquidus temperatures and its comparison with an equilibrium diagram.

EXPERIMENTAL

The following weight compositions were selected for plotting a nonequilibrium diagram and its comparison with an equilibrium one: Ga (I), two hypoeutectic alloys: 95% Ga + 5% Sn (II) and 90% Ga + 10% Sn (III); eutectic alloy 96.3% Ga + 13.7% Sn (IV); and five hypereutectic alloys with tin content: 20% (V), 35% (VI), 50% (VII), 80% (VIII), and pure tin (IX).

The alloys were produced by the melting of gallium and tin (ACS grade) of respective composition with a

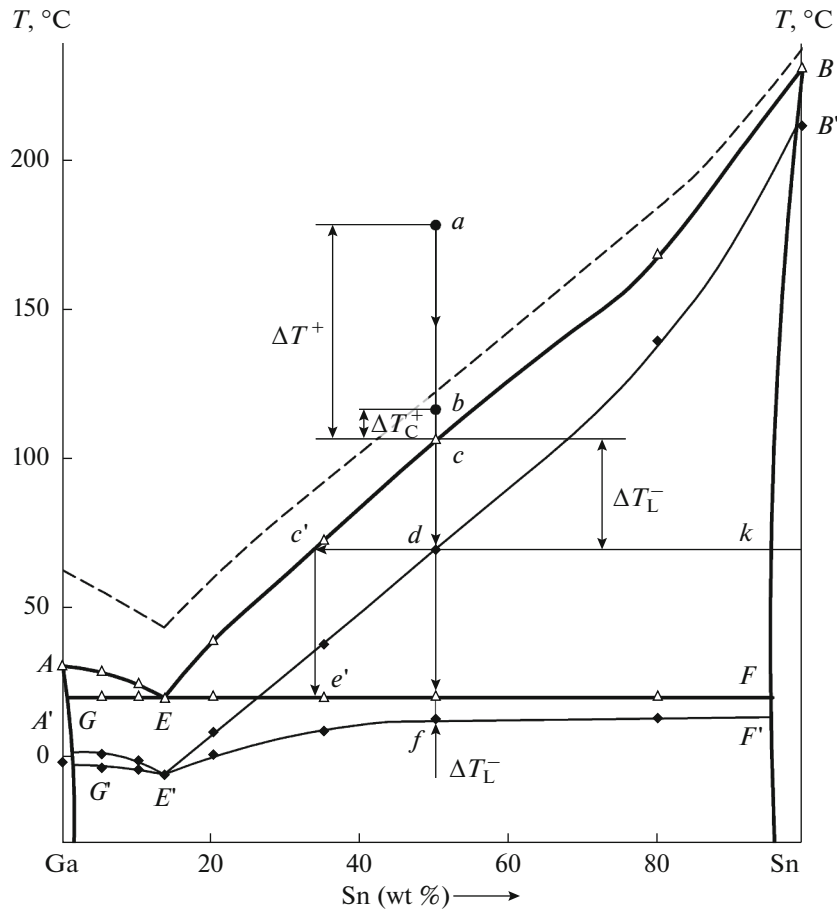


Fig. 1. Gallium–tin state diagram. Bold lines 1: equilibrium diagram [6]; thin lines 2: nonequilibrium diagram based on the experimental data given in this article; and dashed line: conventional boundary of critical overheating of melts. The paths of equilibrium and nonequilibrium crystallization are shown for the 50 wt % Ga + 50 wt % Sn alloy.

total weight of 0.5 g. During melting, the components were heated in an alundum crucible to 282°C, that is, above the melting points of Sn (232°C) and Ga (29.8°C), and mixed up to complete dissolution. The samples were heated and cooled under similar conditions in the so called gradientless resistance furnace. The furnace with a sample was located in a Beko cooling chamber at –30°C. The temperature was measured by a chromel–copel thermocouple using a UT325 digital thermometer connected to a PC. The temperature measurement error was ~0.2°C. Heating and cooling rates were in the range of 3–4°C/min. In certain cases, Ga, Sn, and eutectic alloy were cooled also at a rate of 0.06 and 60°C/min. Three samples of respective composition were analyzed; five thermal cycles of heating and cooling were recorded for each sample. Cyclic thermal analysis is comprised of the continuous recording of thermal cycles of heating and cooling in temperature (T)–time (τ) coordinates in a preset temperature range. The thermograms were analyzed according to the known procedures [14, 15].

The researchers in [16–19] determined two types of crystallization for gallium, tin, and Ga–Sn eutectic

alloy as a function of overheating temperature of the liquid phase and upon subsequent cooling: equilibrium crystallization (EC) without overcooling and nonequilibrium explosive crystallization (NEEC) with overcooling specific for each metal. Critical overheating values (ΔT_C^+) of transition from EC to NEEC were as follows: ~3–4°C for Sn, ~20–22°C for Ga, and ~29–30°C for the eutectic alloy. On the basis of these data, the boundary of critical overheating

$T_C^+ = T_L + \Delta T_C^+$ was outlined for Ga–Sn alloys illustrated by the dashed line in Fig. 1. Such a boundary is also stipulated by the fact that, according to [20, 21], in Ga–Sn alloys in a liquid state, the required overheating above liquidus guarantees that the molten alloy receives a microhomogeneous solution and retains it at any cooling rates. Taking into account the influence of overheating on pre-crystallization overcooling, thermograms of all samples were determined in the temperature range 45°C higher and by 40°C lower than the melting point or the liquidus temperature. Steady overcooling was obtained exactly under these conditions; their values were used to highlight

Table 1. Liquidus and solidus temperatures and respective overcooling in Ga–Sn system

Alloy no.	Composition		$T_L, ^\circ\text{C}$	$T_S, ^\circ\text{C}$	$T_m, ^\circ\text{C}$	$T'_m, ^\circ\text{C}$	$\Delta T_L^-, ^\circ\text{C}$	$\Delta T_S^-, ^\circ\text{C}$
	wt %	mol %						
I	100 Ga	100 Ga?	29.8		–4,2		34	
II	Ga + 5.0 Sn	Ga + 3.0 Sn	25.2	20.5	1.6	–1.1	23.6	21.6
III	Ga + 10.0 Sn	Ga + 6.1 Sn	24.0	20.5	0.3	–3.9	23.7	24.4
IV (E)	Ga + 13.7 Sn	Ga + 8.5 Sn	20.5		–5.5		26.0	
V	Ga + 20.0 Sn	Ga + 12.8 Sn	37.5	20.5	10.1	10.4	27.4	20.9
VI	Ga + 35.0 Sn	Ga + 24.0 Sn	78.0	20.5	43.9	10.3	34.1	10.2
VII	Ga + 50.0 Sn	Ga + 37.0 Sn	105.1	20.5	69.6	12.8	35.5	7.7
VIII	Ga + 80.0 Sn	Ga + 70.1 Sn	166.2	20.5	135.9	13	30.3	7.5
IX	100 Sn	100 Sn?	232.0		219		13	

metastable regions and the construction of a nonequilibrium diagram in the Ga–Sn system. The acquired experimental data were processed in Microsoft Office Excel.

RESULTS AND DISCUSSION

The following data were acquired by experimental thermograph studies: upon heating—melting points of Ga, Sn, and eutectics, temperatures of solidus (T_E) and liquidus (T_L) of the alloys; upon cooling – minimum temperatures (T_m and T'_m) at the start of crystallization of overcooled melts with regard to T_L and T_E , respectively.

Overcooling with regard to T_L was defined as the difference $\Delta T_L^- = T_L - T_m$, and overcooling with regard to T_E was defined as the difference

$\Delta T_E^- = T_E - T'_m$. This is exemplified in Fig. 2 by four thermograms of heating and cooling of gallium I (a), eutectic alloy IV (b), hypereutectic alloy VII (c), and tin IX (d). It should be mentioned that the melting points of gallium, tin, and eutectic alloy, as well as the temperatures of liquidus and solidus, nearly coincided with reference data in the range of ± 0.5 [6]. These data are summarized in Table 1.

The metastability boundary with regard to the temperatures of liquidus and solidus (lines 2 in Fig. 1) were plotted by the points T_m and T'_m . This results in the nonequilibrium diagram shifting downwards with regard to the equilibrium diagram. It can be seen that the lines of nonequilibrium liquidus $A'E'$ and $E'B'$ are shifted with regard to the lines of equilibrium liquidus AE and EB , and the lines of nonequilibrium solidus $G'E'$ and $E'F'$ are shifted with regard to equilibrium solidus GE and EF . Herewith, the eutectics composition is not changed and the temperature in the point E' becomes 26°C lower than that of three-phase equilib-

rium in point E . In the hypoeutectic region, a minor decrease in overcooling is expected, whereas, in the hypereutectic region, their increase upon approaching the eutectic composition of the alloy is expected. This probably can be attributed to the fact that gallium is prone to higher overcooling in comparison with tin. Experiments with Ga, Sn, and eutectic alloy IV at cooling rates of 0.06 and $60^\circ\text{C}/\text{min}$ demonstrated that, upon a variation of cooling rates in this range, the average overcooling with regard to the respective melting point remained nearly the same.

Since the equilibrium crystallization of alloys starts at liquidus temperature T_L and nonequilibrium crystallization at temperature T_m , it would be interesting to analyze the activities of components at these temperatures.

In order to calculate the activity coefficients and the activation energies both under equilibrium and metastable conditions, it was required to estimate the eutectic constituent and solid α , β solutions in melts with eutectics. This was aided by calculating the weight composition of these constituents in the melts.

Let us consider the calculations for alloy VII (50 Sn + 50 Ga, wt %). Amounts of each metal in 0.5 g of liquid alloy are 0.25 g. Since the gallium content in the alloy is lower its content in the eutectics, then all gallium is consumed for the formation of the eutectics. Let us determine the weight of the eutectic alloy; 0.5 g of the eutectic alloy should contain 0.432 g Ga (eut. 13.7 wt % Sn + 86.3 wt % Ga). In the calculations it should be taken into consideration that the Ga–Sn state diagram includes the solubility of Sn in Ga (α solid solution: 0.029 wt %) and Ga in Sn (β solid solution: 4.297 wt %); hence, the eutectic horizontal line would equal not 100 wt %, but 95.67 wt %. With consideration for the data, the proportion will be as follows: $0.863/0.25 = 0.957/X$, from which $X = (0.957 \times 0.25)/0.863 = 0.277$ g (eut.); that is, the alloy 50 wt % Sn + 50 wt % Ga with the weight of 0.5 g con-

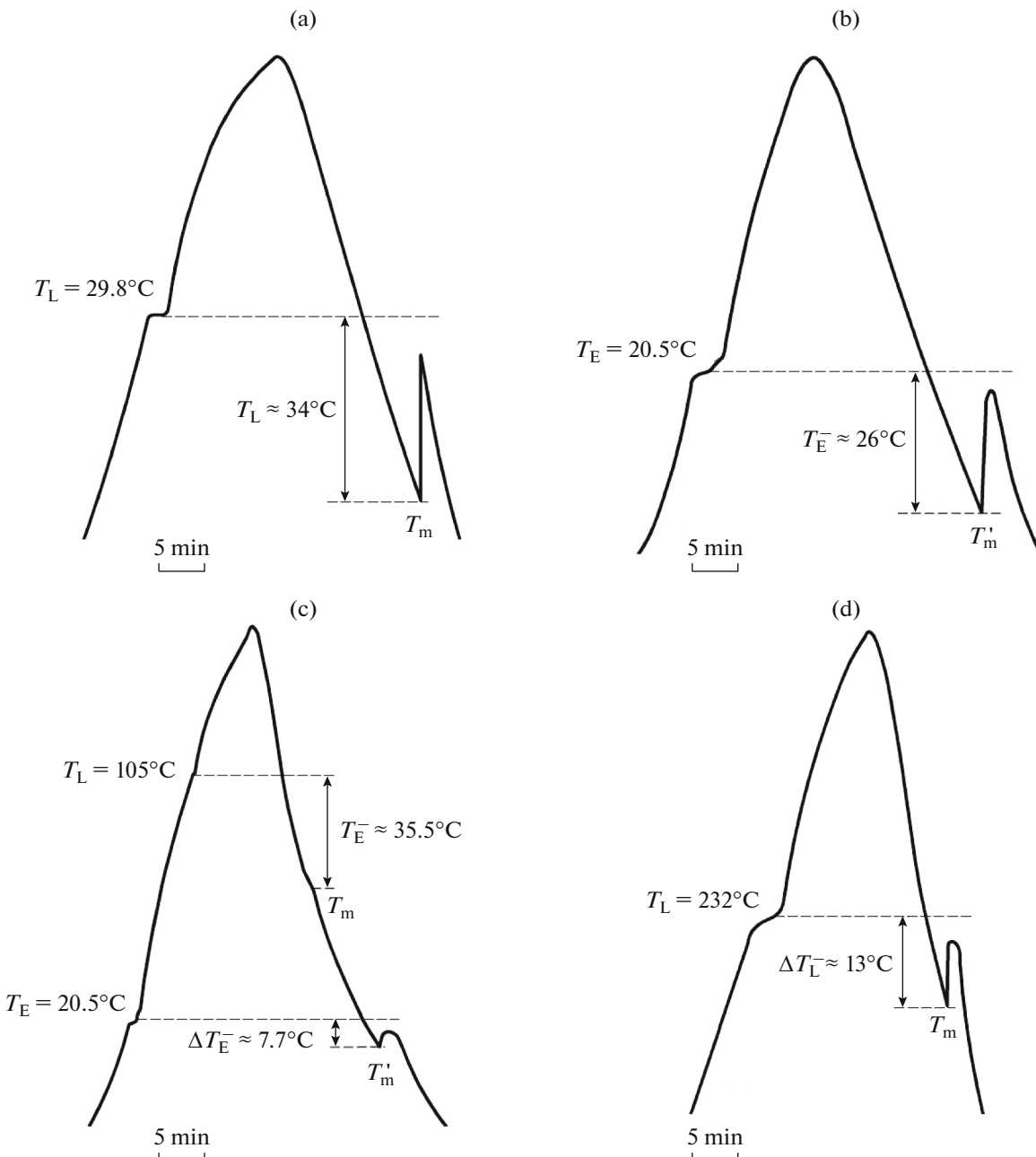


Fig. 2. Heating and cooling thermograms: (a) gallium, (b) eutectic alloy IV, (c) alloy VII, and (d) tin.

tains 0.277 g of eutectics, and the remainder (0.223 g) is β solid solution.

The obtained values of eutectic constituent of the alloys were converted into relative weight and molar concentrations summarized in Table 2. Calculations of the activity coefficients and the activation energies for hypoeutectic alloys were based on the mole composition of α phase (Y_i^α) and those for hypereutectic alloys on the mole composition of β phase (Y_i^β).

The activities of gallium (a_i^{Ga}) and tin (a_i^{Sn}) in the liquid melt at the start of equilibrium crystallization at

T_L (that is, without overcooling) were calculated by the Shreder equation [12]:

(i) for hypoeutectic alloys:

$$a_i^{\text{Ga}} = \exp\left[\frac{\Delta H_L^{\text{Ga}}}{R} \left(\frac{1}{T_L^{\text{Ga}}} - \frac{1}{T_L}\right)\right], \quad (1)$$

(ii) for hypereutectic alloys:

$$a_i^{\text{Sn}} = \exp\left[\frac{\Delta H_L^{\text{Sn}}}{R} \left(\frac{1}{T_L^{\text{Sn}}} - \frac{1}{T_L}\right)\right], \quad (2)$$

Table 2. Relative content of eutectics and α , β phases in alloys with eutectics

Alloy no.	Relative content in alloys with eutectics			
	of eutectics		of α and β phases (Y_i)	
	weight	molar	weight	molar
II	0.349	0.452	0.651	0.548 (α)
III	0.699	0.780	0.301	0.220 (α)
IV (E)	1.0	1.0?	1.0	1.0?
V	0.887	0.923	0.113	0.770 (β)
VI	0.721	0.797	0.279	0.203 (β)
VII	0.554	0.656	0.446	0.344 (β)
VIII	0.222	0.305	0.778	0.695 (β)

where ΔH_L^{Ga} and ΔH_L^{Sn} are the melting enthalpies of gallium (5.59 kJ/mol) and tin (7.07 kJ/mol) [13], T_L^{Ga} and T_L^{Sn} are the melting points of gallium and tin, and $R = 8.31$ J/(mol K). The calculations are based on Kelvin degrees (K).

The activity coefficients of gallium (g_i^{Ga}) and tin (g_i^{Sn}) under the same conditions were determined by the ratios of activities to concentrations of components in respective alloys (Y_i^α , Y_i^β):

$$g_i^{\text{Ga}} = a_i^{\text{Ga}}/Y_i^\alpha, \quad g_i^{\text{Sn}} = a_i^{\text{Sn}}/Y_i^\beta. \quad (3)$$

The activities and the activity coefficients in alloys are summarized in Table 3.

Then (see Table 3), the activation energies both in hypoeutectic (W_i^{Ga}) and in hypereutectic (W_i^{Sn}) alloys were determined as follows [14]:

$$W_i^{\text{Ga}} = \frac{\Delta H_L^{\text{Ga}}(1 - T_L/T_L^{\text{Ga}}) + RT_L \ln Y_i^\alpha}{(1 - Y_i^\alpha)^2}, \quad (4)$$

$$W_i^{\text{Sn}} = \frac{\Delta H_L^{\text{Sn}}(1 - T_L/T_L^{\text{Sn}}) + RT_L \ln Y_i^\beta}{(1 - Y_i^\beta)^2}. \quad (5)$$

The energies W_i^{Ga} and W_i^{Sn} were used to verify the activity coefficients (g_i^{Ga} and g_i^{Sn}) using the procedure in [14]:

$$g_i^{\text{Ga}} = \exp\left[-(1 - Y_i^\alpha)^2 W_i^{\text{Ga}}/(RT_L)\right], \quad (6)$$

$$g_i^{\text{Sn}} = \exp\left[-(1 - Y_i^\beta)^2 W_i^{\text{Sn}}/(RT_L)\right]. \quad (7)$$

The data for g_i^{Ga} and g_i^{Sn} obtained by Eqs. (6), (7) completely coincide with the numerical values obtained by Eq. (3).

Peculiar interest is attracted to an analysis of the aforementioned parameters in the overcooled metastable region at the start of alloy crystallization. Let us denote the activities at the boundary of metastability in the alloy as δ_i^{Ga} , δ_i^{Sn} ; the activity coefficients as γ_i^{Ga} , γ_i^{Sn} ; and the activation energies as ω_i^{Ga} , ω_i^{Sn} . In order to adapt Eqs. (1), (2), (4), (5) to a calculation of the aforementioned parameters for the boundary of metastability of alloys, the boundaries of metastability of gallium and tin should be taken into account. Since in this work gallium, tin, and the considered alloys were crystallized under the same conditions, the respective boundary temperatures can be determined: $T_m^{\text{Ga}} = T_L^{\text{Ga}} - \Delta T_m^{\text{Ga}}$, $T_m^{\text{Sn}} = T_L^{\text{Sn}} - \Delta T_m^{\text{Sn}}$, $T_m^i = T_L^i - \Delta T_L^-$.

Table 3. Activities, activity coefficients, and activation energies for pure Ga, Sn, and their alloys on the lines of equilibrium (a , g , W) and nonequilibrium (δ , γ , ω) liquidus

Alloy no.	Without overcooling			With consideration for overcooling			
	a	g	W , kJ/mol	δ	γ	ω , kJ/mol	
II	0.9663	1.7639	-6.88	1.0233	1.9245	-7.31	
III	0.9575	4.3433	-5.96	1.0439	4.7266	-5.81	
IV	Ga Sn	0.9320	1.0186	-6.22	0.9879	1.0797	-23.59
		0.2970	3.4941	-3.64	0.2343	2.7562	-2.69
V		0.3481	4.5054	-4.56	0.2792	3.6132	-3.55
VI		0.4775	2.3577	-3.93	0.3846	1.8991	-2.66
VII		0.5681	1.6504	-3.66	0.4704	1.3667	-2.07
VIII		0.7769	1.1184	-4.38	0.7037	1.0130	-0.47

In this case the Shreder logarithmic equation can be applied and Eqs. (1), (2), (4), (5) can be rewritten as follows:

$$\delta_i^{\text{Ga}} = \exp \left[\frac{\Delta H_L^{\text{Ga}}}{R} \left(\frac{1}{T_m^{\text{Ga}}} - \frac{1}{T_m^i} \right) \right], \quad (8)$$

$$\delta_i^{\text{Sn}} = \exp \left[\frac{\Delta H_L^{\text{Sn}}}{R} \left(\frac{1}{T_m^{\text{Sn}}} - \frac{1}{T_m^i} \right) \right], \quad (9)$$

$$\omega_i^{\text{Ga}} = \frac{\Delta H_L^{\text{Ga}} \left(1 - T_m^i / T_m^{\text{Ga}} \right) + RT_m^i \ln Y_i^\alpha}{\left(1 - Y_i^\alpha \right)^2}, \quad (10)$$

$$\omega_i^{\text{Sn}} = \frac{\Delta H_L^{\text{Sn}} \left(1 - T_m^i / T_m^{\text{Sn}} \right) + RT_m^i \ln Y_i^\beta}{\left(1 - Y_i^\beta \right)^2}. \quad (11)$$

The activity coefficients of gallium (γ_i^{Ga}) and tin (γ_i^{Sn}) in a metastable region were determined by an equation similar to Eq. (3):

$$\gamma_i^{\text{Ga}} = \delta_i^{\text{Ga}} / Y_i^\alpha, \quad \gamma_i^{\text{Sn}} = \delta_i^{\text{Sn}} / Y_i^\beta. \quad (12)$$

The numerical values of δ_i^{Ga} , δ_i^{Sn} , ω_i^{Ga} , ω_i^{Sn} , γ_i^{Ga} , γ_i^{Sn} are also summarized in Table 3.

It follows from Table 3 that the activities of components both in the line of equilibrium and nonequilibrium liquidus naturally decrease and the activity coefficients increase while the composition approaches the eutectic level.

Finally, let us consider the paths of equilibrium and nonequilibrium crystallization of the alloys. This is exemplified in Fig. 1 by the crystallization paths for alloy VII (Ga + 50 wt % Sn). As was mentioned above, two types of crystallization are possible depending on melt overheating and subsequent cooling: equilibrium one upon cooling, for instance, from the point *b*, and nonequilibrium explosive one upon cooling from the point *a*. In the first case, according to [22], the crystallization path runs across the points $b \rightarrow c \rightarrow c' \rightarrow E$, since the crystallization starts at the liquidus temperature (that is, point *c*). Herewith, the deposition of crystals of β solid solution based on tin occurs. Since the melt is depleted with Sn atoms, the liquid phase is enriched with Ga atoms and its composition with respect to the point *d* will shift from point *c'* to eutectic point *E*. The temperature upon cooling varies across points $b \rightarrow c \rightarrow d \rightarrow e$.

The schematic path of nonequilibrium crystallization depends on its type. Let us consider the variant of crystallization, which can start in imaging point *d*, that is, from the overcooling region. If the heat-release rate significantly exceeds the heat rejection rate, then the temperature (ideally) will vary across points $a \rightarrow d \rightarrow c \rightarrow e$, whereas the crystallization path will be as follows: $a \rightarrow d \rightarrow c' \rightarrow E$. In this case, near point *d* in the overcooled state, the composition of the liquid phase

is the same as in points *a* and *c*, and the degree of freedom *i*, according to the Gibbs' phase rule, will be $i = 2 - 1 + 1 = 2$. If the melt in point *d* or during temperature increase from *d* to *c* is partially crystallized, then the composition of liquid phase in any point between *d* and *c* will correspond to the composition in point *c'*. Herewith, the number of degrees of freedom *i*, as in the case of equilibrium crystallization, will be $i = 2 - 2 + 1 = 1$; that is, the system is univariant and two-phase and the *c'k* conode can be used for determining the compositions of liquid (α_L) and solid (α_S) phases: $\alpha_L = dk/c'k$, $\alpha_S = c'd/c'k$. The conode *EF* (as demonstrated above) can be applied to a determination of the content of eutectics in point *e*: eF/EF , or the composition in the hypereutectic region: eE/EF .

Another variant to denote the crystallization paths is available. According to the cluster coagulation model [11], crystal nuclei should be formed in the overcooled region, since the driving force of crystallization exactly for free Gibbs energies between the liquid and solid phases is a function of overcooling. Therefore, during cooling from point *c* to point *d*, a certain amount of nuclei is accumulated in the melt and the composition of liquid, as in the case of equilibrium crystallization, will vary along the *cc'* line and the crystallization path along the points $a \rightarrow c \rightarrow c' \rightarrow e$.

CONCLUSIONS

A nonequilibrium state diagram of Ga–Sn alloys has been constructed for the first time using thermal analysis. This diagram has been constructed on the basis of overcooling of respective melts obtained under normal conditions. The lines of nonequilibrium liquidus and solidus are shifted in comparison with the equilibrium diagram. Herewith, the eutectic temperature decreases by $\sim 26^\circ\text{C}$.

A procedure is proposed to determine the activities and activity coefficients of components at the start of nonequilibrium crystallization from the region of the metastable state.

CONFLICT OF INTEREST

The authors declare that the presented data do not contain any conflict of interest.

REFERENCES

1. Liang Zhao, Yuming Xing Ze, and Wang Xin Liu, The passive thermal management system for electronic device using low-melting-point alloy as phase change material, *Appl. Therm. Eng.*, 2017, vol. 125, pp. 317–327. <https://doi.org/10.1016/j.applthermaleng.2017.07.004>
2. Krayukhin, V.I., RF Patent C09K3/10, 2009. Krayukhin, V.I., RF Patent 2345865 C2, 2009.
3. Roy, Ch.K., Bhavnani, S., Hamilton, M.C., Wayne, J.R., Knight, R.W., and Harris, D.K., Thermal performance of low melting temperature alloys at the interface be-

- tween dissimilar materials, *Appl. Therm. Eng.*, 2016, vol. 99, pp. 72–79.
<https://doi.org/10.1016/j.applthermaleng.2016.01.036>
4. Chentsov, V.P., Shevchenko, V.G., Mozgovoi, A.G., and Pokrasin, M.A., Density and surface tension of heavy liquid-metal coolants: gallium and indium, *Inorg. Mater.: Appl. Res.*, 2011, vol. 2, no. 5, pp. 468–473.
 5. Ivanova, A.G. and Gerasimov, S.F., Dependence of the phase transition temperature of the eutectic alloy Ga–Zn on its morphology, *Izmer. Tekh.*, 2009, no. 1, pp. 34–37.
 6. *Diagrammy sostoyaniya dvoynykh metallicheskiykh system. Spravochnik* (State Diagrams of Binary Metal Systems. Handbook), Lyakishev, N.P., Ed., Moscow: Mashinostroenie, 1997, vol. 2, pp. 657–658.
 7. Puschin, N.A., Stepanovič, S., and Stajič, V., Über die Legierungen des Galliums mit Zink, Cadmium, Quecksilber, Zinn, Blei, Wismut und Aluminium, *Z. Anorg. Allg. Chem.*, 1932, vol. 209, no. 3, p. 329.
 8. Predel, B., Zustandsdiagramm und eigenschaften von Gallium-Zinn-Legierungen, *J. Less-Common Met.*, 1964, vol. 7, no. 5, pp. 347–355.
 9. Trebuhov, A.A., Sarmurzina, R.K., and Sokolskii, D.V., Study of the physicochemical properties of the gallium-tin system, *Zh. Fiz. Khim.*, 1985, no. 8, pp. 2065–2067.
 10. Brekharya, G.P., Effect of cooling rate onto supercooling of metals and alloys and structure formation, *Extended Abstract of Cand. Sci. (Eng.) Dissertation*, Dnepropetrovsk: Dnepropetrovsk State Univ., 1976.
 11. Aleksandrov, V.D., *Kinetika zarodysheobrazovaniya i massovoi kristallizatsii pereokhlazhdennykh rasplavov i amorfnykh sred* (Kinetics of Nucleation and Mass Crystallization of Supercooled Liquids and Amorphous Media), Donetsk: Donbass, 2011.
 12. Aleksandrov, V.D., UA Patent 83721, 2008.
 13. Perepezko, J.H., Nucleation in undercooled liquids, *Mater. Sci. Eng.*, 1984, vol. 65, no. 1, pp. 125–135.
 14. Šesták, J., *Thermal Analysis: Thermophysical Properties of Solids: their Measurements and Theoretical Thermal Analysis*, Amsterdam, New York: Elsevier Science, 1984.
 15. GOST (State Standard) no. R532933–2009: *Identification of Substances and Materials (Heating and Cooling Curves for TA, DTA, DSC, TGA)*, 2009.
 16. Aleksandrov, V.D. and Frolova, S.A., Effect of the overheating of the gallium melt on its supercooling during solidification, *Russ. Metall. (Engl. Transl.)*, 2014, vol. 2014, no. 1, pp. 14–19.
<https://doi.org/10.1134/S0036029514010042>
 17. Aleksandrov, V.D. and Frolova, S.A., The effect of thermal processing of the liquid phase on the crystallization of alloys in the Sn–Bi system, *Rasplavy*, 2003, no. 3, pp. 14–21.
 18. Aleksandrov, V.D. and Barannikov, V.D., Study of the influence of thermal history of tin and lead drops on their crystallization by cyclic thermal analysis, *Khim. Fiz.*, 1998, vol. 17, no. 10, pp. 140–147.
 19. Aleksandrov, V.D., Frolova, S.A., and Amerkhanova, Sh.K., Solidification of the eutectic Ga–Sn alloy, *Russ. Metall. (Engl. Transl.)*, 2016, vol. 2016, no. 5, pp. 437–442.
<https://doi.org/10.1134/S0036029516050025>
 20. Er-Guang Jia, Ai-Qing Wu, Li-Jun Guo, Liu, C.S., Wen-Jun Shan, and Zhen-Gang Zhu, Experimental evidence of the transformation from microheterogeneous to microhomogeneous states in Ga–Sn melts, *Phys. Lett. A*, 2007, vol. 364, no. 6, pp. 505–509.
<https://doi.org/10.1016/j.physleta.2006.12.048>
 21. Zhao Xiaolin, Bian Xiufang, Wang Changchun, and Li Yunfang, The evolution of coordination structure in liquid GaSn alloy, *Chin. J. Phys.*, 2018, vol. 56, no. 6, pp. 2684–2688.
<https://doi.org/10.1016/j.cjph.2018.10.025>
 22. Stromberg, A.G. and Semchenko, D.P., *Fizicheskaya khimiya* (Physical Chemistry), Moscow: Vysshaya Shkola, 1973.

Translated by I. Moshkin